Highlights

Damping Ratio Identification of a Volumetric Modular High-Rise Building

Hollie Moore, John Hickey, Brian Broderick, Breiffni Fitzgerald

- In situ measurements of the wind-induced vibrations of a modular high-rise building were recorded.
- The natural frequency of the measured building was identified.
- The damping ratio of a modular high-rise building from in-situ measurements was estimated using four OMA techniques.
- A quantification of the uncertainty of the calculated damping ratios is provided.

Damping Ratio Identification of a Volumetric Modular High-Rise Building

Hollie Moore[a,*], John Hickey[a], Brian Broderick[a], Breiffni Fitzgerald[a]

[a] *Department of Civil, Structural and Environmental Engineering, Trinity College Dublin, Ireland*

Abstract

Modular Construction is a rapidly growing construction method being employed in increasingly taller and more slender structures. As this innovative form of construction reaches new heights, it is important to understand the inherent properties which govern the dynamic response. The damping ratio of a structure is a critical value in determining the acceleration response of a building and is best characterised through in situ monitoring. However, there are very limited reports of the damping ratios from modular buildings, resulting in a significant uncertainty in the dynamic response of this form of structure. This paper reports research performed through in situ monitoring of a high-rise modular building, *College Road*, located in Croydon, London, United Kingdom. Details of the modular building and the monitoring set up are presented. The recorded acceleration responses of the structure are discussed and four different OMA methods, the Bayesian Fast Fourier Transform, Random Decrement Technique, Analytical Modal Decomposition Random Decrement Technique and Bootstrapped Analytical Modal Decomposition Random Decrement Technique, are applied in order to obtain estimates of modal properties. Both the Bayesian Fast Fourier Transform and Bootstrapped Analytical Modal Decomposition Random Decrement Technique methods allow for estimates of the uncertainty of the calculated damping ratios, providing greater insight into the dynamic behaviour and the range of possible values. Mixture distributions are generated to account for inter-event variability and allow for assessment of the probability of a damping ratio falling below a specified value. This research advances the limited knowledge surrounding the inherent properties of this new method of high-rise construction,

*mooreho@tcd.ie

enabling better prediction of the dynamic response and assessment of compliance to habitability requirements.

Keywords: Modular Construction, Wind-Induced Acceleration, In-situ Monitoring, Modal Damping Ratio, Uncertainty, Natural Frequency

1. Introduction

Volumetric modular construction has received increased interest in recent years due to the many reported benefits over traditional construction methods including reduced environmental impact, improved quality and accuracy, and speed of construction [1–4]. Whilst modular construction has been traditionally used in temporary, repetitive buildings it is now used more widely in residential accommodation, schools and hospitals [5–9]. Advancements in building technology, software and computational capacity have enabled the construction of increasingly tall buildings. The slender and lightweight nature of many high-rise structures leave them more susceptible to wind-induced vibrations which may compromise occupant comfort; often the governing design criteria for such structures arises in the serviceability limit state due to peak accelerations under wind-induced loading [10–12]. This phenomenon has led to research into the dynamic response of tall, slender structures and suitable control measures, for example [9, 13–16]. Such studies have primarily focused on more traditional construction forms such as steel and reinforced concrete. However, the use of modular construction in high-rise structures is still a novel concept with little research or data available on the global dynamic behaviour of such structures.

The damping ratio is a key indicator of how effectively a structure dissipates vibrational energy and is a fundamental factor in determining a structure's susceptibility to dynamic excitation. While computational models, laboratory studies and empirical data can provide estimates of structural damping, the most reliable way to evaluate true damping ratio values is through modal identification using data from field tests on full-scale finished structures [15, 17–19]. Furthermore, in-situ testing can be used to identify the natural frequency of a structure which provides insight into the stiffness of a modular building and the opportunity for comparison with Finite Element models.

Operational Modal Analysis (OMA) is a method of in-situ testing which takes advantage of the natural excitation of structures under environmental loading, negating the requirement of any artificial excitation [20–23]. As such, OMA is an output only method which captures the dynamic response of a structure using a distributed network of sensors and does not rely on knowledge of the exciting forces. Given the uncontrolled nature of the excitation, it is often recommended that structures are instrumented for prolonged periods of time in order to capture responses experienced under a variety of ambient loading conditions [13, 17, 24, 25]. Requiring only a network of sensors and data-loggers, this form of testing is discreet and can be performed whilst the structure is fully operational [21–23]. The measured output signals captured during monitoring can be processed using output-only modal identification techniques in order to calculate properties of interest [23]. However, many OMA techniques, such as the Random Decrement Technique (RDT) [26] or Stochastic Subspace Identification (SSI) [27] only provide a single estimated value of the inherent property of interest and do not provide a quantification of the uncertainty associated with the calculated value [17]. The inability to statistically examine the reliability of the estimates of damping ratio is a significant limitation of these methods which may result in estimates of the damping ratio which do not accurately reflect the true properties of a building. This is particularly true for structures with closely spaced modes which often have complex acceleration responses that are more difficult to analyse appropriately [28, 29]. Therefore, the development of OMA techniques which enable quantification of uncertainty, particularly for closely spaced modes, is necessary [30].

To the best of the authors' knowledge, only one previous study, by Hickey et al. [31], has reported the damping ratio of high-rise modular buildings. Hickey et al. [31] performed in-situ testing of the 135m tall modular building *Ten Degrees* located in Croydon, London, United Kingdom. In total 10 so-called wind events from two triaxial accelerometers were analysed using three different OMA techniques: the Bayesian Fast Fourier Transform (BFFT), the Random Decrement Technique (RDT) and a hybrid RDT method using Analytical Mode Decomposition (AMD) [32] termed the AMD-RDT [29, 33]. The damping ratio was reported as approximately 1.10%. However, this value only represents the damping ratio of a single modular building. Furthermore, there is no design code which provides a damping ratio value specific to modular construction for use in design [2, 3, 9, 31]. The limited damping ratios reported in literature and design codes mean designers are forced to use estimates based on other forms of construction. For example, the European standard design code, Eurocode 1991-1-4 [34], recommends a value of 0.08 for the logarithmic decrement of damping, equivalent to 1.27% of critical damping, for mixed concrete and steel structures but this value is not specific to modular buildings. It is reasonable to hypothesise that given the many extra connections in a modular building that damping should be greater than in a conventional structure as there is more scope for relative motion and frictional energy dissipation. However this has not yet been investigated by in-situ monitoring. Therefore, it is imperative for the progression of modular buildings that further monioring of this form of construction is performed in order to better understand typical dynamic properties and associated uncertainties.

Building upon the work presented in Hickey et al. [31], this study presents results from further in situ testing of a 163m modular building. Furthermore, it also proposes an improved AMD-RDT method which involves bootstrapping to provide quantification of the uncertainty of damping ratio estimates. The structure studied is *College Road*, located in Croydon, London, United Kingdom in an adjacent site to the previously studied *Ten Degrees*. The paper begins by describing the structural form of *College Road* and the monitoring setup, before the measured acceleration responses of the building for 15 different of 12 hours monitoring periods are presented. Four different OMA techniques are applied, namely the BFFT, RDT, AMD-RDT and hybrid Bootstrapped AMD-RDT method. Estimates of the damping ratios and associated uncertainties obtained from the BFFT and Bootstrapped AMD-RDT OMA methods are reported for each of the events studied. Furthermore, Gaussian mixture probability distributions of the damping ratio are presented, accounting for the aleatory inter-event variability of the damping ratio. These distributions enable assessment of the probability of the damping ratio being less than values of interest, providing a useful tool for determining appropriate values to use in serviceability limit state design of tall modular buildings.

This work not only addresses the knowledge gap surrounding the dynamic response of modular buildings, but also enables quantification of the uncertainty of a key parameter affecting the dynamic response, the damping ratio, through an improved OMA method. These developments aid the design of modular buildings as they continue to increase in height and allow for improved assessment of compliance with habitability requirements in order to ensure occupant comfort.

2. Description of Instrumented Building

Figure 1: *Ten Degrees* (left) and *College Road* (right), Europe's tallest volumetric modular buildings (Source: Tide Construction [35])

The high-rise modular building which has been the subject of full-scale measurements and operational modal analysis is the *College Road* development located in Croydon, London, United Kingdom. *College Road* is a 163 m tall building consisting of two connected towers, a 50-storey tower, Tower A, and a 35-storey tower, Tower B. The structure consists of two slip-formed reinforced concrete (RC) cores, a transfer slab at Level 3 with traditional RC construction below and two adjoined towers of corner post volumetric modules stacked around the RC cores above. Upon completion in 2022 it was the tallest volumetric modular building in Europe [35], surpassing neighbouring *Ten Degrees* by 28 m, which has previously been studied [31]. In the East-West direction the building has a slenderness ratio (Height/Breadth) of 3 and in the North-South direction the slenderness ratio is 8. Figure 1 shows *Ten Degrees* and *College Road* standing side by side.

The two RC cores were treated as the primary lateral stability elements throughout the structural design process, with any lateral stiffness contribution from modules neglected. The RC cores differ in size, with the core of the 35 storey Tower B measuring 8 x 8 m in plan and the core of the 50 storey Tower A measuring 10 x 10 m. The RC cores were constructed via slipforming as free-standing structures, prior to the installation of the modules. This construction process is discussed in more detail in [31]. The modules employed are steel frame volumetric units with a 150 mm thick reinforced concrete slab encased in steel perimeter channels. Modules are designed to support vertical loads, which are carried by four square hollow sections termed 'corner post' columns. It is assumed that all lateral loads are transferred through diaphragm action of the floor slabs back to the RC cores. The member sizes within the modules are highly optimised and change from storey to storey to enhance efficiency and reduce costs.

3. Field Measurements

Field measurements of the ambient acceleration response of *College Road* were recorded continuously for five months during construction, termed Phase 1 of the monitoring campaign, and for a further five months after construction was completed, termed Phase 2. These measurements enabled further study of the dynamic response and inherent modal characteristics of the structure.

Two three-axis MEMS accelerometers, (*LSM6DS3 Inertial Measurement Unit*, resolution 0.00001g, range $\pm$ 2g, frequency range DC 800 Hz) were used to measure the ambient acceleration response. The sampling rates for the accelerometers was 20 Hz. Remote access to the recorded data was enabled by using off-the-shelf smartphones which are manufactured with high specification accelerometers. The devices were given a constant power supply and had 3G fixed wireless internet access. As shown in the left-hand sub-figure of Figure 2, during Phase 1 of monitoring one accelerometer, Accelerometer 1, was placed at the top storey of the core of Tower A and the other, Accelerometer 2, at the top storey of the core of Tower B. Both accelerometers were mounted as close to the centre of the core as possible, approximately 0.8 m above the respective core slab on a rigid, steel post. Although not examining a completed structure, the evolution of modal properties over time can be used to infer the influence of the added modules on structural behaviour. Phase 2 of the monitoring campaign began upon completion of construction. For this phase Accelerometer 2, previously located at the top of Tower B was moved to the top of Tower A, and mounted directly to a module slab at the outer edge of the building, as shown in the right sub-figure of Figure 2. The purpose of this was to provide scope for study of torsional modes. The modal properties identified during this monitoring phase give information about the performance of the completed building.

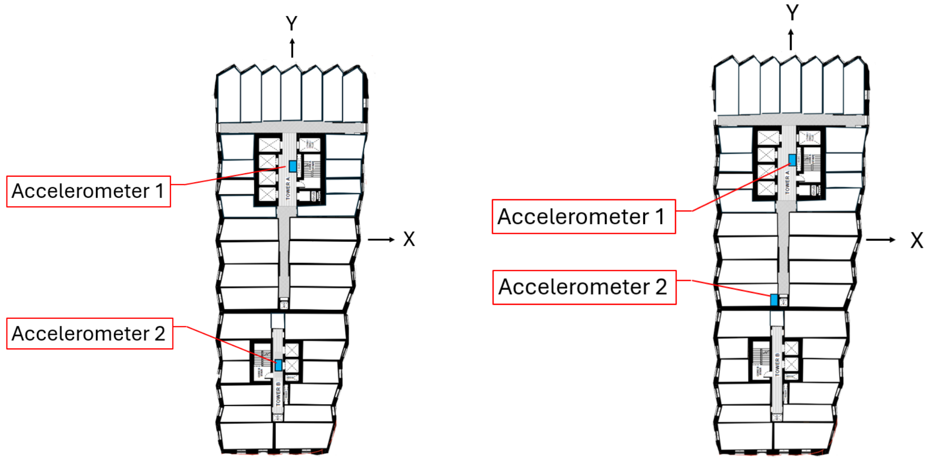

Figure 2: Location of accelerometers during Phase 1 (left) and Phase 2 (right) of the monitoring campaign

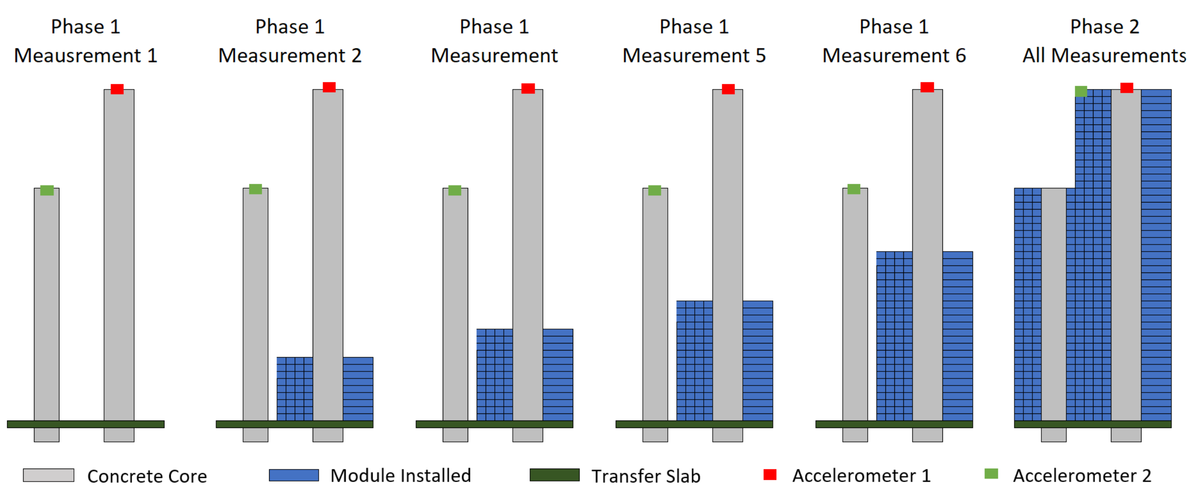

Figure 3: Graphical representation of the number of levels of modules installed at *College Road* for each set event

The reinforced concrete cores were completed in late 2021. The installation of modules in Tower A commenced in November 2021 and in Tower B in May 2022. The initial five months of monitoring, during which modules continued to be installed, took place between December 2021 and April 2022. The first 20 storeys of modules were installed in Tower A during this phase of monitoring and no modules were installed in Tower B. This means Accelerometer 1 on Tower A captured the structural response during the initial stages of module installation. Tower B had no modules installed for the entirety of Phase 1 of the monitoring, meaning the freestanding dynamic response of the RC core was captured by Accelerometer 2.

Installation of the modules was completed in October 2022. The second phase of monitoring began in December 2022 and finished in April 2023. Some construction work, including internal fit out and external cladding installation, was ongoing during this phase of monitoring.

In order to study the building's dynamic response and identify its modal parameters, subsets of the recorded data corresponding to significant wind events were extracted for further study. These monitoring periods were chosen by correlating relatively large acceleration amplitudes in the measurements with wind events noted in meteorological records from Gatwick Airport. Table 1 shows the event number, date and the number of storeys of modules installed in the building at the time of the event. This is visually demonstrated in Figure 3. In total, five acceleration recordings of twelve hours length from each of the accelerometers were selected from the Phase 1 of monitoring during module installation. A sixth shorter event of 3 hours 30 minutes, on 18 February 2022, was also considered. This corresponds to a period of consistently large amplitude accelerations and the highest recorded wind speed during the entire monitoring campaign. However neither the wind speed nor the recorded acceleration are stationary for 12 hours as in other events. A further ten twelve hour measurements were chosen from the data recorded when the structure was fully complete. Power to Accelerometer 2 was interrupted during both the second event in Phase 1 and the last event in Phase 2, meaning data is only available for one accelerometer for these events. All acceleration time series studied are stationary by the both the Augmented Dickey–Fuller [36] and Kwiatkowski–Phillips–Schmidt–Shin tests [37].

The acceleration responses captured during the in-situ monitoring of *College Road* were observed under ambient loading conditions. However, no local measurements of ambient weather conditions were taken. Therefore, the wind speeds during the measured acceleration responses used to identify inherent properties of the structure are unknown. However, records of the wind speed are available for Gatwick Airport, approximately 25 km away from the *College Road* site. These wind speeds are only indicative and are not specific for the site; they are only reported to provide an indication of the regional wind conditions at the time when measurements were recorded. It is important to highlight that the OMA techniques employed in the study are output-only tech-

Event	Start Date	Duration	Number of Storeys Completed		Wind Speed (m/s)		Average Direction
			Tower A	Tower B	Max 10 min Average	Peak Gust	
			Phase 1				
1	07/12/2021 06:00	12 hrs	0	0	8.35	16.09	SE
2	31/01/2022 06:00	12 hrs	9	0	12.98	17.43	NW
3	18/02/2022 12:00	3.5 hrs	13	0	18.55	25.93	WSW
4	20/02/2022 06:00	12 hrs	13	0	11.59	18.33	SW
5	19/03/2022 06:00	12 hrs	17	0	9.27	11.38	ENE
6	07/04/2022 06:00	12 hrs	24	0	16.23	22.80	WSW
			Phase 2				
1	11/01/2023 18:00	12 hrs	50	35	11.59	18.33	SW
2	12/01/2023 18:00	12 hrs	50	35	9.74	17.88	WSW
3	14/01/2023 18:00	12 hrs	50	35	8.35	11.62	WSW
4	17/02/2023 06:00	12 hrs	50	35	8.35	10.73	SW
5	10/03/2023 06:00	12 hrs	50	35	11.13	15.65	NW
6	12/03/2023 18:00	12 hrs	50	35	11.59	16.54	SSW
7	25/03/2023 10:00	12 hrs	50	35	11.13	16.54	WSW
8	29/03/2023 18:00	12 hrs	50	35	9.74	13.41	SSW
9	31/03/2023 10:00	12 hrs	50	35	10.66	15.65	WSW
10	18/04/2023 18:00	12 hrs	50	35	7.88	13.86	SSW

Table 1: Dates of wind events considered, the number of floors of modules installed and indicative wind speed information from nearby Gatwick Airport

niques, so the fact that wind speed was not recorded at the site does not limit their applicability. The peak 10 minute average wind speed, overall peak gust and the average wind direction over the course of the event are presented in Table 1. Only for Event 3 and Event 6 in Phase 1 does the wind speed recorded at Gatwick Airport exceed the 1 in 1 year 10 minute average design wind speed of 16.11 m/s for Serviceability Limit State design. No wind speeds exceeding this design value were recorded during Phase 2 of monitoring.

4. Operational Modal Analysis

The primary purpose of the monitoring of *College Road* was to identify modal parameters of the building. A vast range of OMA techniques are proposed in literature [21, 38]. These include, but are not limited to, time domain techniques such as the random decrement technique [19, 26], stochastic subspace identification (SSI) [27, 39] or the Eigensystem Realization Algorithm (ERA) [40]; frequency domain techniques such as Frequency Domain Decomposition (FDD)[41], Enhanced FDD [42] or the Polyreference Least Squares Complex Frequency method (PolyMAX) [43]; and techniques targeting non-stationary problems that work across both the time and frequency domain such as Wavelet-based approaches [44, 45]. A variety of Bayesian formulations also exist (e.g. [24, 46–49]). Within each of these families of methods, a large number of algorithmic variants, enhancements, developments and combinations of techniques have also been proposed (e.g. [29, 30, 50–56] including in recent years many techniques incorporating clustering or other machine learning techniques (e.g. [57–63]).

This study considers four methods: the Bayesian Fast Fourier Transform (BFFT) which operates in the frequency domain, the Random Decrement Technique (RDT) which operates in the time domain, a hybrid of the RDT which involves first decomposing the response signal into sub-signals using Analytical Mode Decomposition (AMD), hereon referred to as AMD-RDT, and a Bootstrapped version of the combined AMD-RDT method. Both the BFFT method and the developed Bootstrapped AMD-RDT method provide quantification of the error in the estimates of the damping ratio. This is advantageous in determining the reliability of the estimated damping ratio values. Considering both a Bayesian technique and techniques from the RDT family allows results obtained to be compared and cross-validated against one another. This is informative as there can be discrepancies between the estimates returned by different OMA techniques, fundamentally arising from the fact that the damping ratio itself is only an approximate way to quantify the impact of many energy dissipation mechanisms in a structure on vibrational response [19, 64]. However, it is important to state that the purpose of the study is not to compare OMA techniques, hence other equally applicable techniques such as SSI are not applied.

The first method employed to estimate the damping ratio of the structure is the BFFT, which has been used extensively for OMA in previous studies [24, 46–49, 65–68]. The reader is referred to [24] for a detailed explanation of the underlying mathematics. In short, the method uses frequency domain data to maximise the posterior probability density function of the modal parameters and hence, find the most probable value given the measured response. In practice this is achieved by minimizing the negative log-likelihood function. Computationally, this can be challenging, both in terms of time and achieving convergence. Au [47] proposed an efficient method to perform the minimisation where an asymptotic approach can reduce the dimensionality of the minimisation problem and improve computational speed and convergence, which is used in this paper.

The other approaches employed to estimate the damping ratio of the structure are all based on the RDT. This was first proposed for use in the aerospace industry by Cole [26] and has been applied extensively throughout the fields of Civil and Structural Engineering for damping estimation [17, 19, 29, 30, 69]. The RDT can be used to estimate the damping experienced by a linear structural system examining a 'signature' obtained from averaging segments of the response[17, 18]. These segments are sub-sections of the time history of the acceleration response which follow a threshold condition [13, 17, 26, 69], typically a triggering value. By selecting an appropriate trigger value, multiple sub-signals can be obtained. Assuming the forced vibration and the initial velocity of the structure are zero-mean stationary Gaussian variables, averaging across an ensemble of of sub-signals with identical triggering conditions gives only the response due to the initial displacement. Effectively, this means that averaging removes the random component of the response leaving a signal comprising only the free decay response of the structure.

Once the free vibrational response has been determined, the Hilbert transform is applied to the random decrement signature $\delta(t)$ to approximate the free decay response envelope. The damping ratio, ζ_i, is determined by fitting an exponential decay function to this envelope [69, 70]. For multi-degree of freedom systems, simply assuming a Single Degree of Freedom system and applying the RDT, termed the 'traditional RDT' by Tamura et. al [71], can efficiently evaluate the natural frequency and damping ratio if the modes are well separated [71, 72].

While the traditional RDT can work for Multi Degree of Freedom systems if the modes are well separated, in cases with closely located predominant frequency components a beating phenomenon is observed in the random decrement signature and the RDT cannot be used for evaluation of damping ratio [29, 70, 71]. In such cases modal properties can be estimated through superposition of damped free vibration responses, sometimes termed the Multi-Mode Random Decrement technique [72, 73]. Alternatively, this issue can be overcome by combining the RDT with a signal decomposition method. A conceptually straight-forward decomposition approach is to employ a band-pass filter, as in Zhou and Li [17] for example. However it is difficult to design a filter for a complete separation of the two frequency components as the spacing of the two frequencies becomes very small [33]. One potential way to overcome this challenge is through the use of Analytical Mode Decomposition (AMD). This has been shown to be effective for signals with highly coupled modes [28, 32, 33]. In this paper, the AMD is combined with the RDT for modal identification from ambient data as presented by [29, 32]. The AMD decomposes a signal into components separated by a bisecting frequency ω_{bi}, the reader is referred to Chen et al. [32] for details of this process. Other than possible end effects due to the finite length of a structural system's response, the AMD separates the frequency contents of a time series exactly. It has been shown that the selection of the bisecting frequencies does not influence the response decomposition [32, 33], however typically bisecting frequencies are selected around the average of the two adjacent natural frequencies [28, 29, 32, 33]. Once the AMD has been applied, each sub-signal can then be analysed using the RDT to extract the free decay response of the structure and determine its damping ratio. The combination of these approaches is referred to as the AMD-RDT.

In this paper, both the traditional RDT and the AMD-RDT are applied to estimate the damping ratio. However, while use of the RDT is prominent in the literature on modal identification [17, 18, 30], conventional applications do not provide any estimate of uncertainty. To address this deficiency, this paper also employs a hybrid method incorporating the statistical procedure of Bootstrapping within the combined AMD-RDT. This allows a statistical measure of the error in the calculated damping ratio values, and hence, gives an understanding of the uncertainty associated with damping estimates obtained using the AMD-RDT.

Bootstrapping is a statistical procedure involving the resampling of a single dataset to create a number of simulated datasets in which statistical parameters such as standard errors and confidence intervals can be calculated. It has previously been employed with the RDT by Kijewski and Kareeem [74], and others [17]. However this paper considers the combined method of AMD and the RDT, known as the AMD-RDT, merged with bootstrapping to provide estimates of the damping ratio alongside its associated standard error.

The principle of bootstrapping is to treat a sample as though it is the population and randomly sample from this to produce an empirical estimate of the statistic's sampling distribution [17, 74, 75]. The bootstrap procedure is applied in this paper as first presented by Efron et al. [75]:

1. A population of random decrement segments, $X = (x_1,\ x_2,\ \ldots,\ x_n)$, with an ensemble mean, $\hat{x}$, approximating the structure's random decrement signature (i.e. the impulse response function) at the mode of interest, is generated from analysis of the relevant acceleration signal.

2. The population of random decrement segments is sampled with replacement to create a 'bootstrap sample', $X^* = ({x_1}^*,\ {x_2}^*,\ \ldots,\ {x_n}^*)$, with an ensemble mean corresponding to the random decrement signature of the bootstrap sample $\hat{x}^*$

3. The bootstrap operation in step 2 is repeated B times to create a bootstrap ensemble containing B replicates, each with a unique random decrement signature $(\hat{x}^*{}_1,\ \hat{x}^*_2,\ \ldots,\ \hat{x}^*_B)$. The modal damping ratio can be estimated for each random decrement signature, creating an ensemble of damping ratios termed 'bootstrap replicates', denoted $\hat{\zeta}^*_b$.

4. The histogram of the damping ratios can be produced in order to identify the probability density function and hence calculate the bootstrap mean, $\bar{\zeta}^*$, using Eq. 1. The standard deviation and coefficient of variation$s^*{}_\zeta$ can also be found using Eq. 2 and Eq. 3 repectively.

$$\bar{\zeta}^* = \mu\left(\hat{\zeta}^*_b\right) = \frac{1}{B}\sum_{b=1}^{B}\hat{\zeta}^*_b \tag{1}$$

$$\bar{s}^*_\zeta = \sigma\left(\hat{\zeta}^*_b\right) = \sqrt{\frac{1}{B-1}\sum_{b=1}^{B}(\hat{\zeta}^*{}_b - \bar{\zeta}^*)^2} \tag{2}$$

$$CV = \frac{\bar{s}^*_\zeta}{\bar{\zeta}^*} \tag{3}$$

In all applications of the RDT in this paper (traditional, AMD-RDT, AMD-RDT with Bootstrapping) the threshold value for the RDT is set as the standard deviation of the acceleration response; results were found to be insensitive to threshold value employed. The length of each segment is set as fifty times the period of the structure. The segments which form the sample can be overlapping. Known as 'level-crossing overlapping' criterion, this was found to be the criterion that yields the least error by Zhou et al. [17].

In the case of bootstrapping the sample population is then randomly sampled to create a 'bootstrap sample' containing 1000 segments, i.e. $n = 1000$, which preliminary analysis showed was sufficient to return converged damping estimates. This process was repeated 1000 times, i.e. $B = 1000$, to create a set of 1000 bootstrap samples. The RDT is then applied to each bootstrap sample to obtain an estimate of the damping ratio, $\hat{\zeta}^*_b$, known as a bootstrap replicate. Eq. 1 - 3 can then be used to calculate the mean estimate of the damping ratio, $\bar{\zeta}^*_b$, the standard error of the estimate, $\bar{s}^*_\zeta$, and the coefficient of variation, CV.

5. Identification of Modal Properties

5.1. Natural Frequency

Although not the primary focus of this paper, the identified natural frequencies are presented briefly in this section for completeness. Fast Fourier Transforms were performed on each measured ambient acceleration response in order to examine the measured response in the frequency domain.

5.1.1. During Construction

Figure 4 presents an example of the Power Spectral Destiny of the acceleration responses from both accelerometers in both directions for Event 4 in Phase 1 of the monitoring campaign. This is representative of the frequency domain response observed for all events in Phase 1. When considering this information, it is important to bear in mind that this Phase of the monitoring

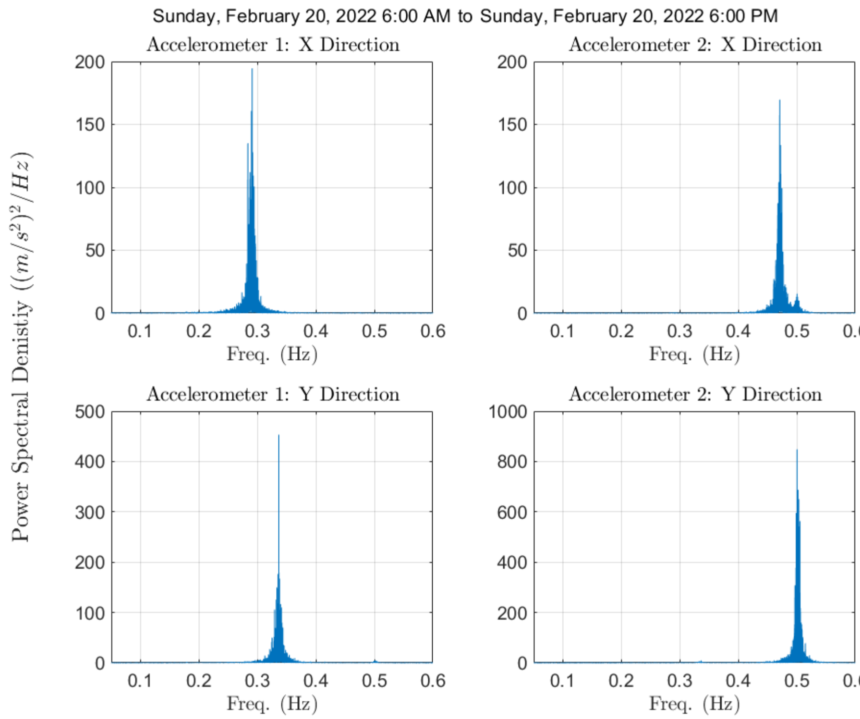

Figure 4: Power Spectral Density of accelerations recorded during Event 4 during Phase 1 of the monitoring campaign

campaign is essentially monitoring two independent structures, as the towers were not connected at this time. For both structures, a first mode is clearly identifiable in the x direction and a second mode with a slightly higher frequency is clear in the y direction. This implies that the mode shapes are closely aligned with the axes of the accelerometers. This pattern, with different modes identifiable from the x and y acceleration recordings, is seen for all events.

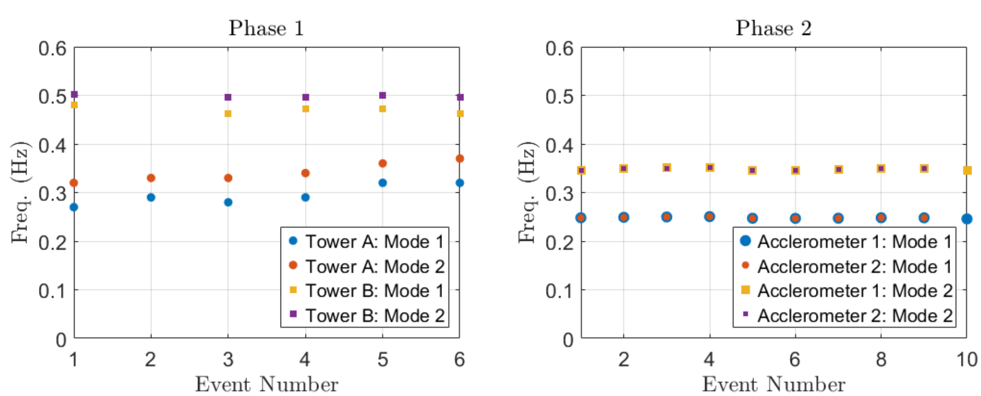

Figure 5: Natural Frequencies of the first two modes identified during Phase 1 and Phase 2 of the monitoring campaign

The left hand sub-figure in Figure 5 shows the natural frequencies obtained for the events studied during the construction of the building. Over the course of this phase of monitoring the structure around Tower A is evolving as more modules are added whereas Tower B is a free-standing core for all events, as illustrated in Figure 3. From Figure 5, it can be appreciated that the natural frequencies of Tower B remain essentially constant through this Phase of monitoring; this is as expected given no modules are added. In contrast, for Tower A the natural frequencies of both modes increase gradually over the course of the monitoring phase. This is attributable to the installation of extra modules to this tower, and indicates that the modules effectively increase the lateral stiffness of the building. This trend is different from that reported in [31], where monitoring during the construction phase showed that frequency decreased as modules were added. This difference is a result of the fact that in [31] modules were added closer to the top of the structure. This suggests that when modules are added near the base the additional stiffness has a greater impact on global characteristics, whereas the additional mass of extra modules becomes more impactful nearer the top of the structure.

5.1.2. Completed Building

Figure 6 presents an example of the Power Spectral Destiny of the acceleration responses from both accelerometers in both directions for Event 6 in Phase 2 of the monitoring campaign, This is typical of the frequency domain response observed in all events for the completed building. When considering results from this Phase it should be borne in mind that, unlike Phase 1, the accelerometers both measure the response of the same building, meaning similar modal properties should be identified from both instruments. The first mode, at approximately 0.248Hz, is clearly identifiable in the acceleration response from the x direction. This mode, as well a second mode, at 0.350Hz, is identifiable in the y acceleration responses.

The right-hand subplot in Figure 5 shows the natural frequencies calculated using the BFFT for each of the acceleration responses from both accelerometers for all events during Phase 2 of the monitoring campaign. It is also possible to obtain the natural frequency from RDT-based methods, but these results are not presented both for brevity and because it can be easily appreciated how the presented values from the BFFT align closely with the values obtained from 'peak-picking'

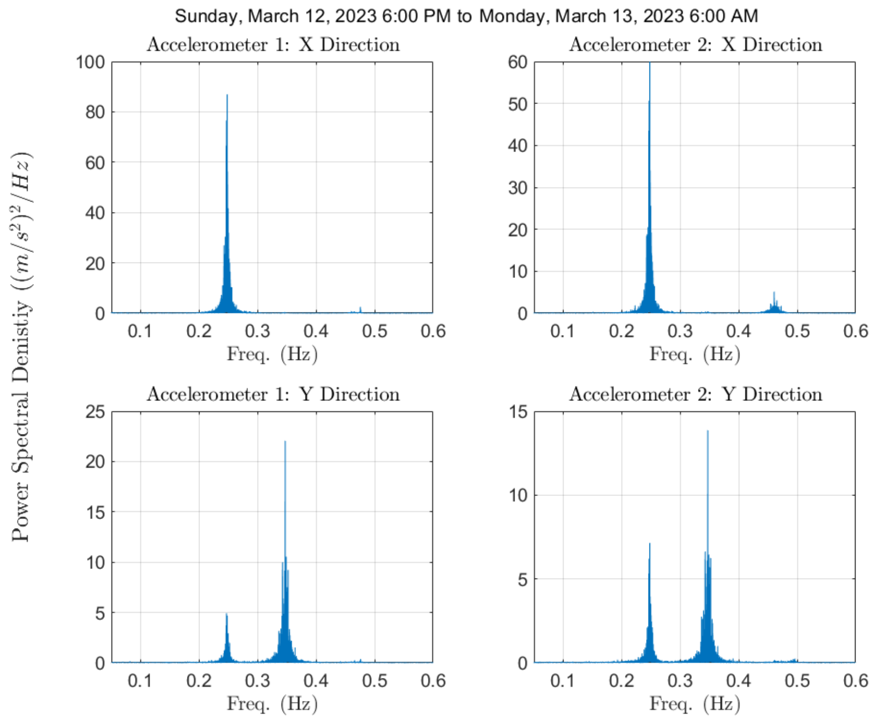

Figure 6: Power Spectral Density of accelerations recorded during Event 6 during Phase 2 of the monitoring campaign

in Figure 6. Overall, it can be concluded that the completed structure has natural frequencies of approximately 0.248Hz and 0.350Hz in the first and second mode respectively. The consistency of these frequencies between events suggest that there is no unexpected or unconventional behaviour that would invalidate the use of conventional OMA techniques for modular construction.

The array of accelerometers employed is not sufficiently distributed over the building height to identify the mode shapes, however it can be inferred that the second mode is approximately aligned with the y (NS) direction from the fact that it is not seen in the measurements recorded in the x (EW) direction. While the first mode is observable in both the x and y recordings, the power spectral density is an order of magnitude greater in the x direction, which implies that the mode shape is roughly aligned with this. Given these inferred mode shapes, the difference in natural frequency between the two modes is as expected, as the depth of the building in the x direction is less than half that of the y direction. This consequent greater flexibility in the x direction explains the lower natural frequency of the first mode.

There is also evidence of a mode between 0.45 and 0.5 Hz in the response of accelerometer 2. Given that this appears in accelerometer 2, at the edge of the floor slab, but is much less prominent in accelerometer 1, located at the centre of the core, it can be inferred that this represents a torsional mode. However, the spectral density of this mode is an order of magnitude lower than the translational modes, suggesting that torsional acceleration is not significant.

5.2. Damping Ratio

The modal damping ratio of the first two modes was calculated for both Phases of the monitoring campaign using each of the four modal identification techniques presented in Section 4.

5.2.1. During Construction

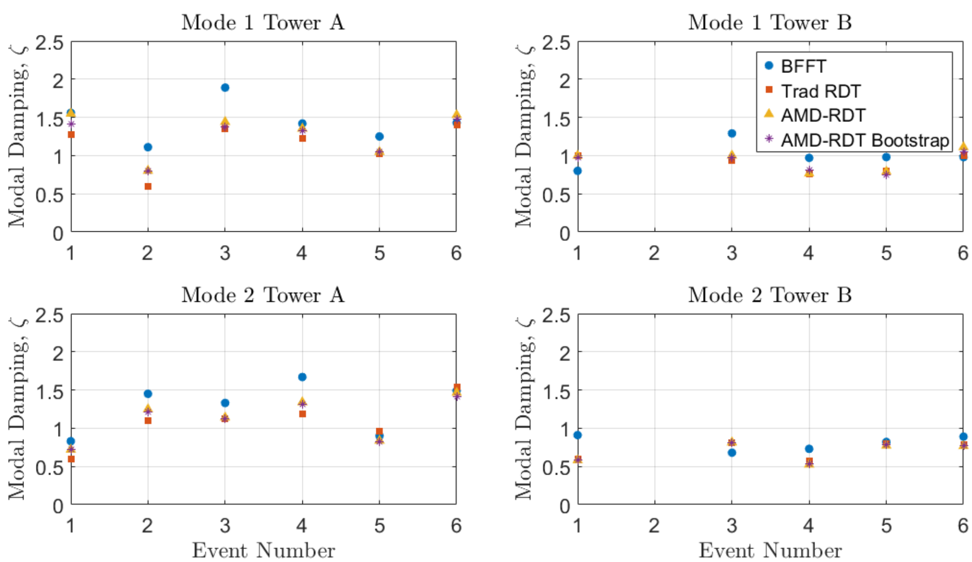

Figure 7: Modal damping ratio of Tower A and Tower B, expressed as a percentage of critical, for each event during Phase 1 of the monitoring campaign

Tables 2 and 3 present the values of modal damping at the first mode estimated from the 6 events during the construction Phase from the four different modal estimation techniques employed. This information is represented graphically in Figure 7.

Considering Tower B firstly, damping ratios in the order of 1% in the first mode and $0.7 - 0.8\%$ in the second mode are observed. These values remain reasonably consistent across events. There is much greater inter-event variability in the data associated with Tower A, as would be expected given that the structure is changing between events. Irrespective of the number of modules installed, estimated damping ratios in Tower A are typically greater than those estimated for Tower B. While this may suggest that modules are contributing additional damping, it should be noted firstly that there are no modules installed in either tower for Event 1, where some of the highest damping values for Mode 1 in Tower A are obtained. Secondly, there is no clearly identifiable trend in damping in Tower A over time as the number of storeys of installed modules increase. Overall, this suggests that the level of modal damping is not necessarily proportional to the number of modules installed and that the number of modules is not the only factor contributing to the difference in observed damping values between Tower A and Tower B.

Table 2: Modal damping ratio of Tower A during construction, expressed as a percentage of critical

Event	Mode 1				Mode 2			
	BFFT	Trad RDT	AMD RDT	AMD RDT Bootstrap	BFFT	Trad RDT	AMD RDT	AMD RDT Bootstrap
1	1.56	1.27	1.55	1.42	0.83	0.60	0.72	0.72
2	1.11	0.60	0.80	0.79	1.45	1.10	1.25	1.21
3	1.89	1.35	1.44	1.38	1.33	1.13	1.14	1.13
4	1.42	1.22	1.35	1.32	1.67	1.18	1.34	1.31
5	1.25	1.02	1.05	1.05	0.9	0.96	0.84	0.83
6	1.43	1.4	1.53	1.48	1.49	1.54	1.47	1.42

Table 3: Modal damping ratio of Tower B during construction, expressed as a percentage of critical

Event	Mode 1				Mode 2			
	BFFT	Trad RDT	AMD RDT	AMD RDT Bootstrap	BFFT	Trad RDT	AMD RDT	AMD RDT Bootstrap
1	0.80	1.00	1.00	0.98	0.91	0.60	0.58	0.59
2	-	-	-	-	-	-	-	-
3	1.29	0.94	1.00	0.97	0.68	0.81	0.81	0.81
4	0.97	0.75	0.77	0.81	0.73	0.57	0.52	0.54
5	0.98	0.80	0.79	0.75	0.82	0.80	0.77	0.78
6	0.98	0.99	1.11	1.05	0.89	0.78	0.77	0.77
Average	1.00	0.90	0.93	0.91	0.80	0.71	0.69	0.70

5.2.2. *Completed Building*

Tables 4 to 7 present the results for each of the events considered in Phase 2 of the monitoring campaign using the various identification techniques. Damping in the first mode is estimated from the accelerations recorded in the x direction (approximately East West), while the second mode is estimated from the accelerations in the y direction (approximately North South). This information is represented graphically in Figure 8.

Isolation of the individual modes in the y direction is achieved via the AMD for the AMD-RDT techniques. This decomposes signals into precise frequency bands; in this case band-limited signals of 0.235 Hz to 0.265 Hz and 0.33 Hz to 0.37 Hz are considered for the first and second modes respectively. For the BFFT, the two modes are deemed to be well-separated based on the definition of well-separated modes provided by Au [47], as the frequency bands in question are each dominated by a single mode and the trough between resonant peaks in the Power Spectral Density drops to a similar level to the background noise, as shown in Figure 6. This allows the BFFT technique to be applied for each mode individually, in this case using the same frequency bands as the AMD-RDT. The selection these frequency bands was validated though preliminary analysis which showed that for frequency bands of this approximate magnitude the values of damping ratio estimated from both techniques was insensitive to the exact bandwidth selected.

Table 4: Modal damping ratio of the competed structure, expressed as a percentage of critical, calculated using the BFFT for each event during Phase 2 of the monitoring campaign

Event	Accelerometer 1		Accelerometer 2	
	Mode 1	Mode 2	Mode 1	Mode 2
1	1.38	1.37	1.37	1.37
2	1.37	1.36	1.38	1.38
3	0.99	1.36	0.99	1.39
4	1.04	1.35	1.07	1.44
5	1.17	1.56	1.19	1.5
6	1.12	1.32	1.12	1.35
7	1.12	1.34	1.11	1.36
8	1.12	1.29	1.13	1.38
9	1.07	1.19	1.10	1.22
10	1.08	1.31		
Average	1.15	1.35	1.16	1.38

Table 5: Modal damping ratio of the competed structure, expressed as a percentage of critical, calculated using the traditional RDT for each event during Phase 2 of the monitoring campaign

Event	Accelerometer 1		Accelerometer 2	
	Mode 1	Mode 2	Mode 1	Mode 2
1	1.33	2.08	1.40	2.02
2	1.16	1.84	1.24	1.82
3	1.01	1.72	0.93	1.71
4	0.97	1.84	0.93	1.89
5	0.95	2.37	0.97	2.34
6	1.11	2.00	1.09	1.97
7	1.04	1.81	1.02	1.91
8	1.25	1.64	1.18	1.75
9	1.04	1.55	1.03	1.52
10	1.05	1.61		
Average	1.09	1.85	1.09	1.88

Table 6: Modal damping ratio of the competed structure, expressed as a percentage of critical, calculated using the AMD-RDT for each event during Phase 2 of the monitoring campaign

Event	Accelerometer 1		Accelerometer 2	
	Mode 1	Mode 2	Mode 1	Mode 2
1	1.3	1.36	1.38	1.41
2	1.33	1.24	1.31	1.22
3	0.92	1.26	0.93	1.28
4	0.86	1.22	0.80	1.24
5	0.99	1.74	1.08	1.68
6	1.16	1.38	1.17	1.5
7	1.16	1.15	1.18	1.17
8	1.22	1.14	1.09	1.11
9	0.88	1.29	1.01	1.2
10	0.91	1.27		
Average	1.07	1.24	1.11	1.31

Several comments can be made considering these results. Firstly, considering the average values across events, all four identification techniques return similar values, with the exception of the traditional RDT for the second mode. All techniques identify the damping ratio for the first mode as slightly above 1%. There is also good agreement between the accelerometers with almost identical values estimated from both accelerometer 1 and accelerometer 2 for each technique. This is as expected given that both instruments measured the response of a single structure in this Phase. For the second mode, there is again good agreement between the BFFT and the two AMD-based

Table 7: Mean modal damping ratio of the competed structure, expressed as a percentage of critical, calculated using the AMD-RDT with Bootstrapping for each event during Phase 2 of the monitoring campaign

Event	Accelerometer 1		Accelerometer 2	
	Mode 1	Mode 2	Mode 1	Mode 2
1	1.28	1.31	1.36	1.37
2	1.29	1.17	1.28	1.20
3	0.9	1.22	0.92	1.24
4	0.85	1.2	0.79	1.22
5	0.96	1.61	1.03	1.57
6	1.15	1.34	1.14	1.46
7	1.15	1.14	1.16	1.16
8	1.18	1.12	1.07	1.09
9	0.88	1.25	1.00	1.18
10	0.89	1.24		
Average	1.05	1.26	1.08	1.28

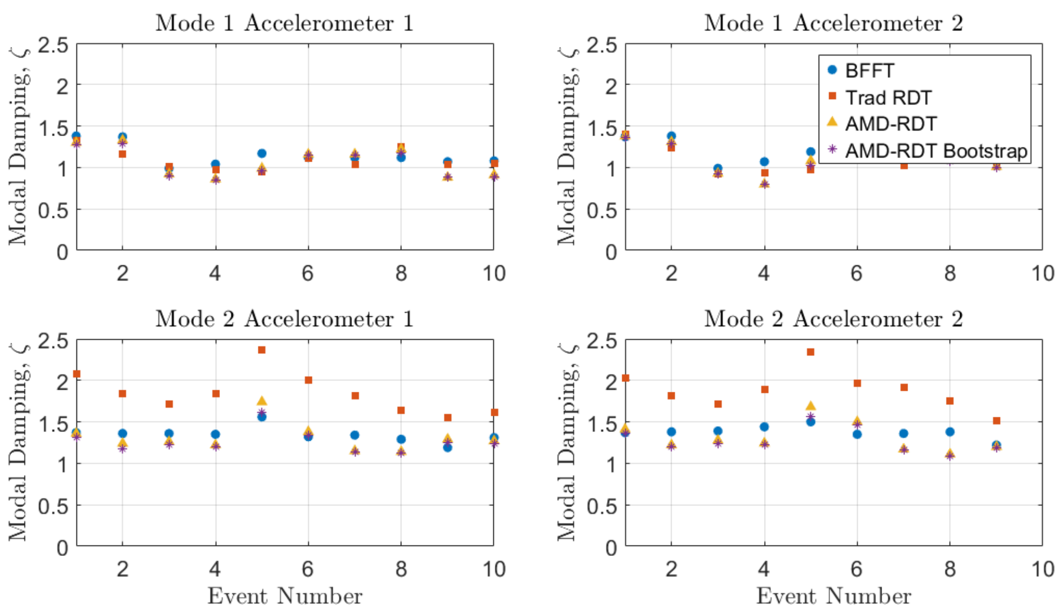

Figure 8: Estimated damping ratios of the completed *College Road* building during Phase 2 of the monitoring calculated using the four different operational modal analysis approaches

techniques, which all return average values of roughly 1.3% for both accelerometers. However, the traditional RDT returns substantiality higher values of 1.85% and 1.88%. Given this difference and the known limitations of the traditional RDT for MDOF systems, these values are likely overestimates. Overall, neglecting the traditional RDT result, it can be concluded that the modal damping ratios are approximately 1.10% and 1.30% in the first and second modes respectively.

There is some variability in the identified damping ratios between events. Event 1 and 2 for mode 1 and Event 5 for mode 2 display slightly greater values than the other events, irrespective of the identification technique employed. The tendency for modal parameters to vary over time is well established in literature and can be seen in the results reported in many OMA studies detailing various in-situ monitoring campaigns (e.g. [76–82]). This variation can arise from a combination of changing ambient conditions, measurement noise and estimation errors [83, 84].

In terms of variability between identification methods, the BFFT approach generally returns slightly higher damping ratios in the majority of cases (again ignoring the traditional RDT results for the second mode). However, the BFFT results also tend to be more consistent and display less inter-event variability than the RDT-based methods. The difference between the damping estimates from the AMD-RDT and BFFT approaches is not statistically significant. P-values of 0.06 (accelerometer 1, mode 1), 0.32 (accelerometer 1, mode 2), 0.13 (accelerometer 2, mode 1) and 0.26 (accelerometer 2, mode 2) are obtained from paired T-tests comparing the two data sets. All of these can be deemed not statistically significant at a significance level of 5%. Furthermore, it is worth noting that in previous work, the BFFT tended to return slightly lower estimates of damping than the RDT-based approaches. Therefore, at least in the absence of more data, it can be concluded that the apparent tendency for the BFFT to return slightly greater values is not systematic.

In general, the modal damping ratios reported here align closely with the damping ratios previously reported by Hickey at al. [31] for the similar *Ten Degrees* modular building. In that study, which as previously mentioned examined a similar but slightly shorter building, damping in the first two modes was reported to be between 1.0% and 1.1% for the first mode and 1.0% and 1.3% for the second mode. In terms of code provisions, Eurocode 1991-1-4 suggests using damping ratios of 0.8% and 1.27% for steel and mixed steel and concrete buildings, respectively. The values recorded in this study, and in [31], agree reasonably well with the value suggested for mixed buildings. However, given the similarity of the results between the monitoring campaigns detailed here and in [31], it may be advisable to conservatively assume a lower value in design of modular structures employing similar core-based structural schemes.

A further important conclusion that can be made from the identified damping values is that there is no evidence to support the hypothesis that damping ratios may be higher in modular buildings than in conventional construction. Modular buildings are characterized by a large number of joints and interfaces between modules and, in the case of the College Road development, between modules and the core. Given that it is well known that motion at joints like these can be a major source of frictional energy dissipation in structural dynamics, it is reasonable to suspect that, given the much greater number of joints and subsequent potential sources of energy dissipation, damping ratios may be greater in modular buildings. However, the results from monitoring reported here and in [31] suggest that, at least for the levels of excitation broadly typical of serviceability level events, there is no evidence that this is the case. The fact that Phase 1 of the monitoring campaign did not show a consistent increase in damping in Tower A with the addition of modules also supports this conclusion - if modules were adding substantial energy dissipation capability the damping ratios would be expected to increase consistently as more modules are installed. Therefore, at least in the absence of further data, it can be concluded tall modular buildings should not be designed assuming greater levels of damping to conventional steel or steel and concrete buildings.

5.3. Variation of Damping Ratio with Response Amplitude

Previous studies have shown that the level of damping in a structure can depend on response amplitude, with the damping ratio tending to increase with response up to a critical value, for example as discussed in [16, 85–88] amongst other studies. This relationship is explored in this section.

Figure 9 shows damping ratios obtained using the BFFT and AMD-RDT plotted against the root mean square (RMS) acceleration values for each event. Linear trend lines are fitted to the data through robust regression. From this, it can be seen visually that there is some positive correlation between the level of damping and the RMS response for the first mode, but that this relationship is not seen for the second mode. Details of these trend lines are given in the figure which presents the equation, the coefficient of determination (R^2) and the p-value of the slope for each case. For mode 1, for both the AMD-RDT and the BFFT, the trend lines have a positive slope of very approximately $1\%/milli - g$. The p-values are all less than 0.05, suggesting that the identified relationship is statistically significant, i.e. the null hypothesis that damping does not change with RMS acceleration can be rejected. However, the R^2 values, which range between 0.46 and 0.58 are not particularly high, meaning that changes in damping ratio between events cannot be attributed solely to the change in RMS acceleration. It can also be observed from Figure 9 that there is some suggestion that the damping ratio may be reaching a critical value at the higher RMS values, however there is insufficient data to confirm this. In contrast, for the second mode, the p-values of the slope of the regression lines are all greater than 0.05, meaning that the relationship between RMS acceleration and damping is not statistically significant.

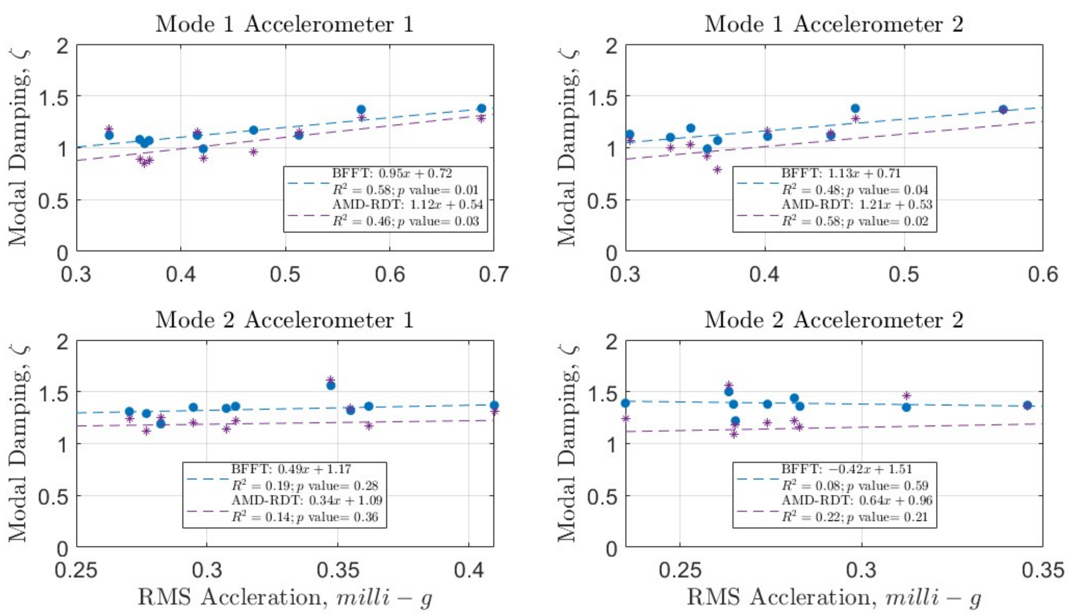

Figure 9: Relationship between estimated modal damping and RMS acceleration

This indicates that there is some relationship between damping ratio and response amplitude, which is to be expected given the results of previous studies. However, response amplitude alone does not explain the variation in estimated damping between events, as shown by the low R^2 values of fitted trend lines and lack of a trend in the second mode. While analysing the impact of response amplitude on modal characteristics it should be borne in mind that the monitoring campaign does not cover the full range of wind speeds or response amplitudes that may be experienced. This is a limitation of the study; while the results here can be used to inform serviceability limit state design, further work is needed to establish damping ratios under more extreme wind speeds.

6. Uncertainty of Damping Ratio Estimates

The standard deviations and coefficient of Variation (CV) of the damping estimates were calculated using the BFFT and Bootstrapped AMD-RDT methods in order to provide an estimate of the uncertainty associated with the estimation of damping. Table 8 show the CV of each estimate of the modal damping ratio in Phase 2 from the BFFT and Bootstrapped AMD-RDT methods. These results are presented graphically in Figure 10. It should be noted that these measures of dispersion consider data from single events only. Therefore, they only represent epistemic uncertainty associated with estimation of the modal damping ratio for a given event, and do not quantify aleatory inter-event variability.

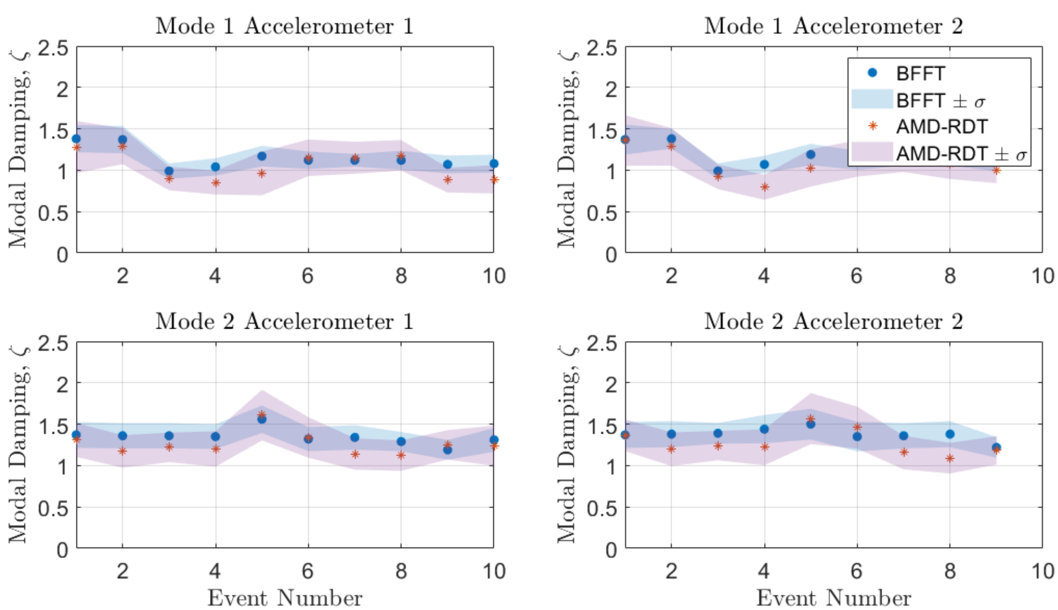

Figure 10: Comparison of damping estimates and their possible range using CV values from both the BFFT and Bootstrapped AMD-RDT method

Aleatory variability across the ensemble of distributions for each event can be quantified using a mixture distribution. For each event, the mean and CV value define a single Gaussian distribution $p(\zeta|e_i)$, conditional on the occurrence of the i^{th} event, e_i. Therefore, the various events lead to a set of distributions, which can be combined to form an overall mixture distribution. This mixture

Table 8: CV of estimates of the damping ratio of from Phase 2 of the monitoring campaign

Event	Accelerometer 1				Accelerometer 2			
	BFFT Mode 1	AMD-RDT Mode 1	BFFT Mode 2	AMD-RDT Mode 2	BFFT Mode 1	AMD-RDT Mode 1	BFFT Mode 2	AMD-RDT Mode 2
1	0.059	0.123	0.057	0.078	0.066	0.113	0.057	0.07
2	0.06	0.084	0.056	0.084	0.043	0.088	0.057	0.085
3	0.047	0.079	0.056	0.073	0.047	0.08	0.045	0.071
4	0.05	0.084	0.055	0.089	0.049	0.095	0.059	0.089
5	0.053	0.137	0.053	0.095	0.054	0.11	0.062	0.098
6	0.047	0.096	0.055	0.091	0.051	0.096	0.066	0.087
7	0.034	0.084	0.055	0.083	0.025	0.078	0.056	0.087
8	0.051	0.078	0.045	0.082	0.032	0.083	0.057	0.085
9	0.050	0.085	0.05	0.071	0.051	0.078	0.051	0.072
10	0.050	0.096	0.054	0.098				

distribution can be calculated as a weighted sum of the n different conditional distributions:

$$p(\zeta) = \sum_{i=1}^{n} w_i p(\zeta|e_i) \tag{4}$$

Figure 11 shows the resulting mixture distributions obtained from the results of the BFFT and Bootstrapped AMD-RDT respectively. In the development of these mixture distributions each mixture component is weighted equally, i.e. $w_i = \frac{1}{n}$. It can be appreciated that the resulting mixture distributions are not normal and in some cases are multi-modal, behaviour which is common for Gaussian mixture distributions. The expected value, i.e. mean, $E[\zeta] = \frac{1}{n}\sum E[\zeta|e_i]$, and standard deviation, $\sigma = \sqrt{E[\zeta^2] - E[\zeta]^2}$, of these mixture distributions can be calculated and are presented in Figure 11. The expected values of damping across the ensemble of events obtained from the two modal identification techniques are similar, within 0.1% of one another in all cases, however the values returned by the BFFT are slightly higher. From examining the distributions visually it can be observed that the spread of the estimates from the Bootstrapped AMD-RDT method is greater than the BFFT. This is also reflected in the greater standard deviations. An explanation for this lies in the BFFT being Bayesian method, where the width of the distributions obtained reduces as the amount of data increases. This does not happen for uncertainty estimation techniques based on

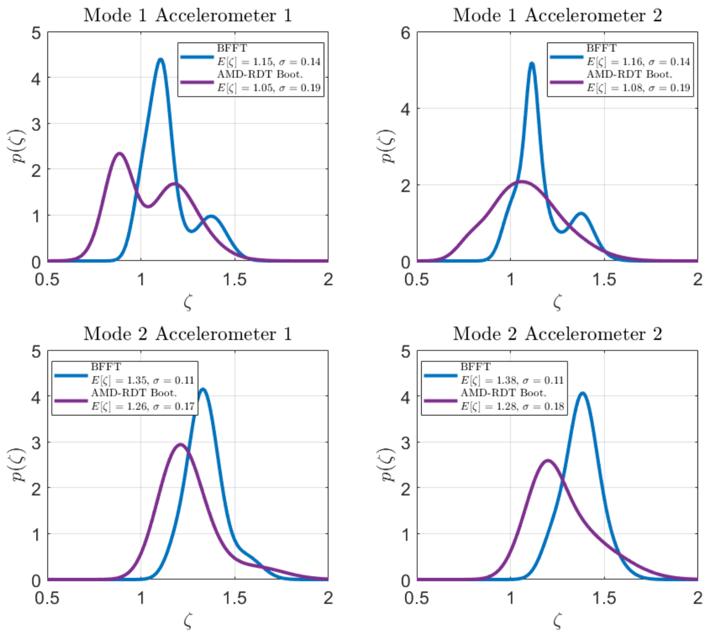

Figure 11: Mixture probability density functions, $p(\zeta)$, for modal damping calculated from BFFT and Bootstrapped AMD RDT estimates of damping for individual wind events

bootstrapping, which quantify sampling variability rather than parameter uncertainty. Cumulative probability distributions can also be calculated, allowing the probability of exceeding damping values of interest to be assessed, as shown in Figure 12. For example, the probability of modal damping being less than 1.0% and the recommended value of 1.27% in Eurocode 1991-1-4 are presented in Figure 12. Examining these probabilities, it can be seen that the probability of damping being less than 1.27% is estimated to be in the order of 0.8, meaning that a lower value is more appropriate for serviceability limit state design.

The ability to quantify uncertainty associated with a given damping value better equips engineers to make informed decisions about the true damping ratio of a structure and it's dynamic response. In turn, this enables improved design and reliability-based assessment of a structure's adherence to habitability requirements and enhances decisions relating to measures necessary to ensure occupant comfort such as inclusion of supplementary damping devices [9]. Furthermore, it gives insight into the level of uncertainty associated with the damping ratio estimates provided here, advancing knowledge about the inherent properties of modular construction. The Bootstrapped

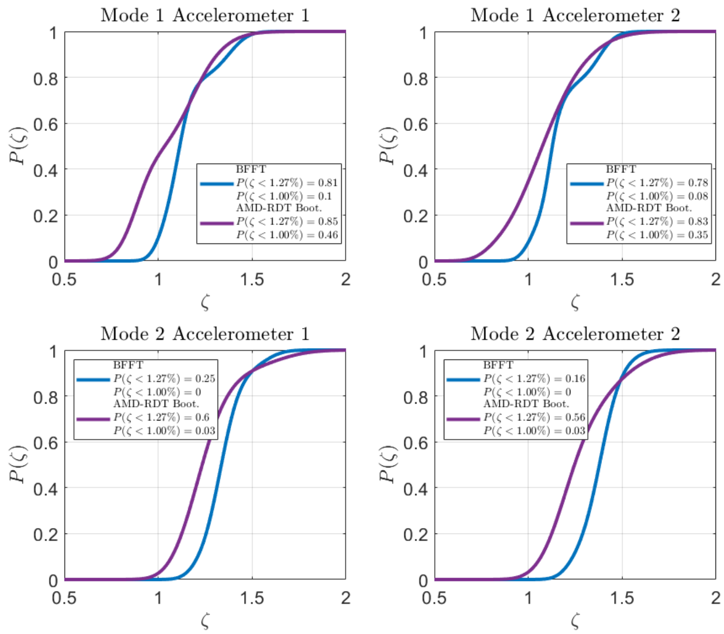

Figure 12: Mixture cumulative distribution functions, $P(\zeta)$, for modal damping calculated from BFFT and Bootstrapped AMD RDT estimates of damping for individual wind events

AMD-RDT method applied here is particularly useful for this purpose as it allows uncertainty in damping ratio estimates to be quantitated for structures with closely spaced modes.

7. Conclusions

This study has detailed the in-situ monitoring of the 163m tall modular high-rise building known as *College Road* located in Croydon, London. The structure was monitored for a period of 5 months during construction and a further period of 5 months after completion. The primary focus of the monitoring campaign was to identify the modal damping ratio, as this is unknown for tall modular buildings. Four different OMA techniques were used to calculate the modal properties: the BFFT, RDT, AMD-RDT and Bootstrapped AMD-RDT.

The natural frequency of the first two modes of the completed building were found to be $0.248Hz$ and $0.350Hz$ respectively. Modal damping ratios varied slightly between both events and identification techniques, with values identified using the BFFT method being slightly greater than those identified using the RDT, AMD-RDT and Bootstrapped AMD-RDT methods. However, on average this modal damping was found to be slightly above 1.0% for the first mode and approximately 1.3% for the second mode.

Uncertainty in these estimates was further explored for the BFFT and Bootstrapped AMD-RDT methods. This was done firstly by examining the uncertainty associated with the estimation of damping for individual events using the coefficient of variation and then by considering inter-event uncertainty through the development of mixture distributions. For the data examined it was found that the spread of the values from the Bootstrapped AMD-RDT values is greater than the BFFT. Furthermore, the probability of damping being less than various damping ratios of interest was assessed. From this, it was shown that the probability of damping being less than the value of 1.27% recommended by Eurocode for mixed steel and concrete buildings is in the order of 0.8 and that a lower value may be more appropriate for use in the serviceability limit state design of tall modular buildings.

More generally, this research has given valuable insights into the inherent properties of a high-rise modular building. The damping ratios reported add to those previously reported by Hickey et al. [31] and help to create a database of empirical damping estimates for modular construction, similar to those available for more traditional forms of construction.The identified damping ratios and associated errors can be used in the design of future volumetric modular buildings, providing engineers with more knowledge to make informed decisions about the dynamic behaviour to ensure occupant comfort.

Despite this, there remains a need for further in-situ monitoring of tall modular structures to validate the conclusions of this work. In particular, there is a need to study damping ratios at higher response amplitudes. While it should be borne in mind that the wind speeds reported are only indicative and not site specific, the values experienced during the monitoring campaign were relatively low. The results reported here suggest that damping levels may increase under greater response amplitude, however further work is needed to verify this trend and establish a suitable damping value for ultimate limit state design. Furthermore, as tall modular construction becomes more common, it is necessary to monitor and report modal parameters for a wider range of buildings in order to assess to what extent the conclusions reported here can be generalized.

Acknowledgements

Funding for this research was provided by the Irish Government through the Irish Research Council [Grant No. EBPPG/2020/244] and by Barrett Mahony Consulting Engineers. Information and data collection for this research was facilitated and supplied by Tide Construction. The authors also wish to thank Shane Linehan and Vincent Barrett at Barrett Mahony Consulting Engineers for their support in this work.

Author contributions: CRediT

Hollie Moore: Data curation, Formal analysis, Writing – original draft; **John Hickey:** Conceptualization, Formal analysis, Writing – original draft; **Brian Broderick:** Writing – review and editing, Funding acquisition, Supervision; **Breiffni Fitzgerald:** Writing – review and editing, Funding acquisition, Supervision

References

[1] M. Lawson, R. Ogden, and C. Goodier, *Design in Modular Construction*. CRC Press, 2014.

[2] Z. Chen, K. Khan, A. Khan, K. Javed, and J. Liu, "Exploration of the multidirectional stability and response of prefabricated volumetric modular steel structures," *Journal of Constructional Steel Research*, vol. 184, p. 106826, 2021. [Online]. Available: https://www.sciencedirect.com/science/article/pii/S0143974X21003084

[3] H.-T. Thai, T. Ngo, and B. Uy, "A review on modular construction for high-rise buildings," *Structures*, vol. 28, pp. 1265–1290, 2020. [Online]. Available: https://www.sciencedirect.com/science/article/pii/S2352012420305476

[4] T. Gunawardena, T. Ngo, P. Mendis, and J. Alfano, "Innovative flexible structural system using prefabricated modules," *Journal of Architectural Engineering*, vol. 22,

no. 4, p. 05016003, 2016. [Online]. Available: https://doi.org/10.1061/(ASCE)AE.1943-5568.0000214

[5] M. J. Hough and R. M. Lawson, "Design and construction of high-rise modular buildings based on recent projects," in *Proceedings of the Institution of Civil Engineers-Civil Engineering*, vol. 172. Thomas Telford Ltd, 2019, pp. 37–44. [Online]. Available: https://doi.org/10.1680/jcien.18.00058

[6] W. Ferdous, Y. Bai, T. D. Ngo, A. Manalo, and P. Mendis, "New advancements, challenges and opportunities of multi-storey modular buildings – a state-of-the-art review," *Engineering Structures*, vol. 183, pp. 883–893, 2019. [Online]. Available: http://www.sciencedirect.com/science/article/pii/S0141029618334175

[7] R. M. Lawson, R. G. Ogden, and R. Bergin, "Application of modular construction in high-rise buildings," *Journal of Architectural Engineering*, vol. 18, no. 2, pp. 148–154, 2012. [Online]. Available: https://doi.org/10.1061/(ASCE)AE.1943-5568.0000057

[8] J. Y. R. Liew, Y. S. Chua, and Z. Dai, "Steel concrete composite systems for modular construction of high-rise buildings," *Structures*, vol. 21, pp. 135–149, 2019. [Online]. Available: https://www.sciencedirect.com/science/article/pii/S2352012419300347

[9] J. Hickey, B. Broderick, B. Fitzgerald, and H. Moore, "Mitigation of wind induced accelerations in tall modular buildings," *Structures*, vol. 37, pp. 576–587, 2022. [Online]. Available: https://www.sciencedirect.com/science/article/pii/S2352012422000376

[10] Y. Tamura, "Application of damping devices to suppress wind-induced responses of buildings," *Journal of Wind Engineering and Industrial Aerodynamics*, vol. 74-76, pp. 49–72, 1998. [Online]. Available: https://www.sciencedirect.com/science/article/pii/S0167610598000063

[11] *ISO 10137: Basis for Design Structures : Serviceability of Buildings and Walkways Against*

Vibrations. British Standard, 2007. [Online]. Available: https://books.google.ie/books?id=nYWzzQEACAAJ

[12] *Guidelines for the Evaluation of Habitability to Building Vibration*. Architectural Institute of Japan, 1991.

[13] T. Kijewski-Correa, J. Kilpatrick, A. Kareem, D.-K. Kwon, R. Bashor, M. Kochly, B. S. Young, A. Abdelrazaq, J. Galsworthy, and N. Isyumov, "Validating wind-induced response of tall buildings: Synopsis of the Chicago full-scale monitoring program," *Journal of Structural Engineering*, vol. 132, no. 10, pp. 1509–1523, 2006. [Online]. Available: https://ascelibrary.org/doi/abs/10.1061/%28ASCE%290733-9445%282006%29132%3A10%281509%29

[14] T. Ohkuma, H. Marukawa, Y. Niihori, and N. Kato, "Full-scale measurement of wind pressures and response accelerations of a high-rise building," *Journal of Wind Engineering and Industrial Aerodynamics*, vol. 38, no. 2, pp. 185–196, 1991. [Online]. Available: https://www.sciencedirect.com/science/article/pii/0167610591900404

[15] R. Smith, R. Merello, and M. Willford, "Intrinsic and supplementary damping in tall buildings," *Proceedings of the Institution of Civil Engineers - Structures and Buildings*, vol. 163, no. 2, pp. 111–118, 2010. [Online]. Available: https://www.icevirtuallibrary.com/doi/abs/10.1680/stbu.2010.163.2.111

[16] Y. Tamura and A. Yoshida, "Amplitude dependency of damping in buildings," in *Structures Congress 2008*, 2008, pp. 1–10. [Online]. Available: https://doi.org/10.1061/41000(315)39

[17] K. Zhou and Q.-S. Li, "Reliability analysis of damping estimation by random decrement technique for high-rise buildings," *Earthquake Engineering and Structural Dynamics*, 2020. [Online]. Available: http://dx.doi.org/10.1002/eqe.3396

[18] Q. Li, K. Zhou, and X. Li, "Damping estimation of high-rise buildings considering structural

modal directions," *Earthquake Engineering and Structural Dynamics*, vol. 49, no. 6, pp. 543–566, 2020. [Online]. Available: https://doi.org/10.1002/eqe.3253

[19] A. Kareem and K. Gurley, "Damping in structures: its evaluation and treatment of uncertainty," *Journal of Wind Engineering and Industrial Aerodynamics*, vol. 59, no. 2, pp. 131–157, 1996. [Online]. Available: https://www.sciencedirect.com/science/article/pii/0167610596000049

[20] O. Avci, K. Alkhamis, O. Abdeljaber, A. Alsharo, and M. Hussein, "Operational modal analysis and finite element model updating of a 230 m tall tower," *Structures*, vol. 37, pp. 154–167, 2022. [Online]. Available: https://www.sciencedirect.com/science/article/pii/S2352012421011966

[21] E. Reynders, "System identification methods for (operational) modal analysis: Review and comparison," *Archives of Computational Methods in Engineering*, vol. 19, no. 1, pp. 51–124, 2012. [Online]. Available: https://dx.doi.org/10.1007/s11831-012-9069-x

[22] C. Rainieri and G. Fabbrocino, "Operational modal analysis: overview and applications," *Strategies for reduction of the seismic risk*, pp. 29–44, 2008.

[23] F. B. Zahid, Z. C. Ong, and S. Y. Khoo, "A review of operational modal analysis techniques for in-service modal identification," *Journal of the Brazilian Society of Mechanical Sciences and Engineering*, vol. 42, no. 8, 2020. [Online]. Available: https://dx.doi.org/10.1007/s40430-020-02470-8

[24] S.-K. Au, "Fast Bayesian ambient modal identification in the frequency domain, part i: Posterior most probable value," *Mechanical Systems and Signal Processing*, vol. 26, pp. 60–75, 2012. [Online]. Available: https://www.sciencedirect.com/science/article/pii/S0888327011002391

[25] J. Zhang and Q. Li, "Wind tunnel test and field measurement study of wind effects on

a 600-m-high super-tall building," *The Structural Design of Tall and Special Buildings*, vol. 26, no. 17, p. e1385, 2017. [Online]. Available: https://doi.org/10.1002/tal.1385

[26] H. Cole, "On-line failure detection and damping measurement of aerospace structures by random decrement signatures," no. NASA-CR-2205. NASA, March 1973. [Online]. Available: https://ntrs.nasa.gov/citations/19730010202

[27] B. Peeters and G. De Roeck, "Reference-based stochastic subspace identification for output-only modal analysis," *Mechanical systems and signal processing*, vol. 13, no. 6, pp. 855–878, 1999. [Online]. Available: https://doi.org/10.1006/mssp.1999.1249.

[28] Z.-C. Wang and G.-D. Chen, "Analytical mode decomposition of time series with decaying amplitudes and overlapping instantaneous frequencies," *Smart Materials and Structures*, vol. 22, no. 9, p. 095003, jul 2013. [Online]. Available: https://doi.org/10.1088/0964-1726/22/9/095003

[29] Q. Wen, X. Hua, Z. Chen, H. Niu, and X. Wang, "AMD-based random decrement technique for modal identification of structures with close modes," *Journal of Aerospace Engineering*, vol. 31, no. 5, p. 04018057, 2018. [Online]. Available: https://ascelibrary.org/doi/abs/10.1061/%28ASCE%29AS.1943-5525.0000882

[30] Z. Feng, B. Zhao, X. Hua, Z. Chen, and M. Asce, "Enhanced EMD-RDT method for output-only ambient modal identification of structures," *Journal of Aerospace Engineering*, vol. 32, p. 04019046, 2019. [Online]. Available: https://ascelibrary.org/doi/abs/10.1061/%28ASCE%29AS.1943-5525.0001034

[31] J. Hickey, H. Moore, B. Broderick, and B. Fitzgerald, "Structural damping estimation from live monitoring of a tall modular building," *The Structural Design of Tall and Special Buildings*, vol. 33, no. 1, p. e2067, 2024. [Online]. Available: https://onlinelibrary.wiley.com/doi/abs/10.1002/tal.2067

[32] G. Chen and Z. Wang, "A signal decomposition theorem with hilbert transform and its application to narrowband time series with closely spaced frequency components," *Mechanical Systems and Signal Processing*, vol. 28, pp. 258–279, 2012. [Online]. Available: https://www.sciencedirect.com/science/article/pii/S0888327011000641

[33] Z. Wang and G. Chen, "Analytical mode decomposition with Hilbert transform for modal parameter identification of buildings under ambient vibration," *Engineering Structures*, vol. 59, pp. 173–184, 2014. [Online]. Available: https://www.sciencedirect.com/science/article/pii/S0141029613004872

[34] *Eurocode 1: Actions on structures - Part 1-4: General actions - Wind actions*. European Committee for Stadarization, 2004, no. EN 1991-1-4:2005. [Online]. Available: https://eurocodes.jrc.ec.europa.eu/EN-Eurocodes/eurocode-1-actions-structures

[35] Tide Construction. (2024) College road. [Online]. Available: https://tideconstruction.co.uk/projects/college-road/

[36] D. A. Dickey and W. A. Fuller, "Likelihood ratio statistics for autoregressive time series with a unit root," *Econometrica: journal of the Econometric Society*, pp. 1057–1072, 1981.

[37] D. Kwiatkowski, P. C. Phillips, P. Schmidt, and Y. Shin, "Testing the null hypothesis of stationarity against the alternative of a unit root: How sure are we that economic time series have a unit root?" *Journal of econometrics*, vol. 54, no. 1-3, pp. 159–178, 1992.

[38] R. Brincker and C. Ventura, *Introduction to operational modal analysis*. John Wiley & Sons, 2015.

[39] P. Van Overschee and B. De Moor, "Subspace algorithms for the stochastic identification problem," *Automatica*, vol. 29, no. 3, pp. 649–660, 1993. [Online]. Available: https://www.sciencedirect.com/science/article/pii/000510989390061W

[40] J.-N. Juang and R. S. Pappa, “An eigensystem realization algorithm for modal parameter identification and model reduction,” *Journal of guidance, control, and dynamics*, vol. 8, no. 5, pp. 620–627, 1985.

[41] R. Brincker, L. Zhang, and P. Andersen, “Modal identification from ambient responses using frequency domain decomposition,” in *IMAC 18: Proceedings of the International Modal Analysis Conference (IMAC), San Antonio, Texas, USA, February 7-10, 2000*, 2000, pp. 625–630.

[42] R. Brincker, L. Zhang, and P. Andersen, “Modal identification of output-only systems using frequency domain decomposition,” *Smart materials and structures*, vol. 10, no. 3, p. 441, 2001.

[43] B. Peeters, H. Van der Auweraer, P. Guillaume, and J. Leuridan, “The polymax frequency-domain method: a new standard for modal parameter estimation?” *Shock and Vibration*, vol. 11, no. 3-4, pp. 395–409, 2004.

[44] B. F. Yan, A. Miyamoto, and E. Brühwiler, “Wavelet transform-based modal parameter identification considering uncertainty,” *Journal of Sound and Vibration*, vol. 291, no. 1, pp. 285–301, 2006. [Online]. Available: https://www.sciencedirect.com/science/article/pii/S0022460X05003913

[45] C.-S. Huang and W. Su, “Identification of modal parameters of a time invariant linear system by continuous wavelet transformation,” *Mechanical Systems and Signal Processing*, vol. 21, no. 4, pp. 1642–1664, 2007.

[46] K. Yuen and L. S. Katafygiotis, “Bayesian time–domain approach for modal updating using ambient data,” *Probabilistic Engineering Mechanics*, vol. 16, no. 3, pp. 219–231, 2001. [Online]. Available: https://www.sciencedirect.com/science/article/pii/S0266892001000042

[47] S.-K. Au, “Fast Bayesian FFT method for ambient modal identification with separated modes,” *Journal of Engineering Mechanics - ASCE*, vol. 137, no. 3, pp. 214–226,

2011. [Online]. Available: https://ascelibrary.org/doi/abs/10.1061/%28ASCE%29EM.1943-7889.0000213

[48] K.-V. Yuen and L. S. Katafygiotis, "Bayesian fast Fourier transform approach for modal updating using ambient data," *Advances in Structural Engineering*, vol. 6, no. 2, pp. 81–95, 2003. [Online]. Available: https://doi.org/10.1260/136943303769013183

[49] K.-V. Yuen, *Bayesian methods for structural dynamics and civil engineering*. John Wiley and Sons, 2010.

[50] E. Reynders and G. De Roeck, "Reference-based combined deterministic–stochastic subspace identification for experimental and operational modal analysis," *Mechanical Systems and Signal Processing*, vol. 22, no. 3, pp. 617–637, 2008.

[51] L. Zhang, T. Wang, and Y. Tamura, "A frequency–spatial domain decomposition (FSDD) method for operational modal analysis," *Mechanical systems and signal processing*, vol. 24, no. 5, pp. 1227–1239, 2010. [Online]. Available: https://www.sciencedirect.com/science/article/pii/S0888327009003744

[52] J.-S. Hwang, D.-K. Kwon, and A. Kareem, "Frequency domain state space–based mode decomposition framework," *Journal of Engineering Mechanics*, vol. 145, no. 7, p. 04019051, 2019.

[53] C. Xiong, M. Wang, and W. Chen, "Data-driven structural dynamic characteristics investigation by combining RDT and IVMD method," *Structures*, vol. 55, pp. 2295–2306, 2023. [Online]. Available: https://www.sciencedirect.com/science/article/pii/S2352012423009219

[54] P. Ni, Z. Yin, Q. Han, and X. Du, "Output-only structural identification with random decrement technique," in *Structures*, vol. 51. Elsevier, 2023, pp. 55–66.

[55] P. Górski, “Improving the applicability of RDM in identification of multimode structural damping with reduced RD signature quality,” *Journal of Structural Engineering*, vol. 149, no. 5, p. 05023001, 2023.

[56] B. J. O’Connell, M. D. Champneys, and T. J. Rogers, “A new perspective on Bayesian operational modal analysis,” *Mechanical Systems and Signal Processing*, vol. 236, p. 112949, 2025.

[57] F. Magalhães, A. Cunha, and E. Caetano, “Online automatic identification of the modal parameters of a long span arch bridge,” *Mechanical Systems and Signal Processing*, vol. 23, no. 2, pp. 316–329, 2009. [Online]. Available: https://www.sciencedirect.com/science/article/pii/S0888327008001301

[58] E. Reynders, J. Houbrechts, and G. De Roeck, “Fully automated (operational) modal analysis,” *Mechanical systems and signal processing*, vol. 29, pp. 228–250, 2012.

[59] M. Civera, V. Mugnaini, and L. Zanotti Fragonara, “Machine learning-based automatic operational modal analysis: A structural health monitoring application to masonry arch bridges,” *Structural Control and Health Monitoring*, vol. 29, no. 10, p. e3028, 2022.

[60] H. B. Shim, H. S. Park *et al.*, “SSI-LSTM network for adaptive operational modal analysis of building structures,” *Mechanical Systems and Signal Processing*, vol. 195, p. 110306, 2023.

[61] J. Mao, X. Su, H. Wang, and J. Li, “Automated Bayesian operational modal analysis of the long-span bridge using machine-learning algorithms,” *Engineering Structures*, vol. 289, p. 116336, 2023.

[62] W.-H. Feng, C.-Y. Wu, J.-Y. Fu, C.-T. Ng, and Y.-C. He, “Automatic modal identification via eigensystem realization algorithm with improved stabilization diagram technique,” *Engineering Structures*, vol. 291, p. 116449, 2023.

[63] J. Shu, C. Zhang, Y. Gao, and Y. Niu, “A multi-task learning-based automatic blind identification procedure for operational modal analysis,” *Mechanical Systems and Signal Processing*, vol. 187, p. 109959, 2023.

[64] J. Woodhouse, “Linear damping models for structural vibration,” *Journal of Sound and Vibration*, vol. 215, no. 3, pp. 547–569, 1998. [Online]. Available: https://www.sciencedirect.com/science/article/pii/S0022460X98917096

[65] Y.-C. Ni and F.-L. Zhang, “Fast Bayesian frequency domain modal identification from seismic response data,” *Computers and Structures*, vol. 212, pp. 225–235, 2019. [Online]. Available: https://www.sciencedirect.com/science/article/pii/S0045794917314128

[66] S.-K. Au and F.-L. Zhang, “Ambient modal identification of a primary–secondary structure by Fast Bayesian FFT method,” *Mechanical Systems and Signal Processing*, vol. 28, pp. 280–296, 2012. [Online]. Available: https://www.sciencedirect.com/science/article/pii/S0888327011002962

[67] S.-K. Au, F.-L. Zhang, and Y.-C. Ni, “Bayesian operational modal analysis: Theory, computation, practice,” *Computers and Structures*, vol. 126, pp. 3–14, 2013. [Online]. Available: https://www.sciencedirect.com/science/article/pii/S0045794912003288

[68] X. Qing, M. F. Huang, W. Lou, and Y. Ni, “Modal identification of Canton Tower using the fast Bayesian FFT method,” *Smart Structures and Systems*, vol. 10, pp. 353–373, 2012. [Online]. Available: https://doi.org/10.12989/sss.2012.10.4_5.353

[69] T. Kijewski and A. Kareem, “Reliability of random decrement technique for estimates of structural damping,” in *8th ASCE Specialty Conference on Probabilistic Mechanics and Structural Reliability*, 2000, pp. 294–299.

[70] J. N. Yang, Y. Lei, S. Lin, and N. Huang, “Identification of natural frequencies and dampings of in situ tall buildings using ambient wind vibration data,” *Journal of engineering*

mechanics, vol. 130, no. 5, pp. 570–577, 2004. [Online]. Available: https://ascelibrary.org/doi/abs/10.1061/%28ASCE%290733-9399%282004%29130%3A5%28570%29

[71] Y. Tamura, A. Yoshida, L. Zhang, T. Ito, S. Nakata, and K. Sato, "Examples of modal identification of structures in Japan by FDD and MRD techniques," in *Proceedings of the 1st International Operational Modal Analysis Conference, IOMAC 2005*, 2005, Conference Proceedings. [Online]. Available: https://www.iomac.info/iomac2005

[72] Y. Tamura, L. Zhang, A. Yoshida, S. Nakata, and T. Itoh, "Ambient vibration tests and modal identification of structures by FDD and 2DOF-RD technique," *The Proceedings of the Symposium on the Motion and Vibration Control*, vol. 2003.8, 2002.

[73] Y. Tamura, A. Yoshida, and L. Zhang, "Evaluation techniques of damping in buildings," in *CTBUH 2004 World Congress, Seoul, Korea*, 2004, pp. 158–165.

[74] T. Kijewski and A. Kareem, "On the reliability of a class of system identification techniques: insights from bootstrap theory," *Structural Safety*, vol. 24, no. 2, pp. 261–280, 2002. [Online]. Available: https://www.sciencedirect.com/science/article/pii/S0167473002000280

[75] B. Efron and R. Tibshirani, "Bootstrap methods for standard errors, confidence intervals, and other measures of statistical accuracy," *Statistical Science*, vol. 1, no. 1, pp. 54–75, 1986. [Online]. Available: http://www.jstor.org/stable/2245500

[76] S. Alampalli, "Effects of testing, analysis, damage, and environment on modal parameters," *Mechanical Systems and Signal Processing*, vol. 14, no. 1, pp. 63–74, 2000. [Online]. Available: https://www.sciencedirect.com/science/article/pii/S0888327099912712

[77] P. Cornwell, C. R. Farrar, S. W. Doebling, and H. Sohn, "Environmental variability of modal properties," *Experimental techniques*, vol. 23, no. 6, pp. 45–48, 1999. [Online]. Available: https://onlinelibrary.wiley.com/doi/abs/10.1111/j.1747-1567.1999.tb01320.x

[78] B. Peeters and G. De Roeck, “One-year monitoring of the Z24-Bridge: environmental effects versus damage events,” *Earthquake engineering & structural dynamics*, vol. 30, no. 2, pp. 149–171, 2001. [Online]. Available: https://onlinelibrary.wiley.com/doi/abs/10.1002/1096-9845%28200102%2930%3A2%3C149%3A%3AAID-EQE1%3E3.0.CO%3B2-Z

[79] K.-V. Yuen and S.-C. Kuok, “Modeling of environmental influence in structural health assessment for reinforced concrete buildings,” *Earthquake Engineering and Engineering Vibration*, vol. 9, no. 2, pp. 295–306, 2010. [Online]. Available: https://doi.org/10.1007/s11803-010-0014-4

[80] P. Moser and B. Moaveni, “Environmental effects on the identified natural frequencies of the Dowling Hall Footbridge,” *Mechanical Systems and Signal Processing*, vol. 25, no. 7, pp. 2336–2357, 2011. [Online]. Available: https://www.sciencedirect.com/science/article/pii/S0888327011001233

[81] A. Bajrić, J. Høgsberg, and F. Rüdinger, “Evaluation of damping estimates by automated operational modal analysis for offshore wind turbine tower vibrations,” *Renewable Energy*, vol. 116, pp. 153–163, 2018. [Online]. Available: https://www.sciencedirect.com/science/article/pii/S0960148117302355

[82] D. Hwang, S. Kim, and H.-K. Kim, “Long-term damping characteristics of twin cable-stayed bridge under environmental and operational variations,” *Journal of Bridge Engineering*, vol. 26, no. 9, p. 04021062, 2021. [Online]. Available: https://ascelibrary.org/doi/abs/10.1061/%28ASCE%29BE.1943-5592.0001761

[83] I. Behmanesh, B. Moaveni, G. Lombaert, and C. Papadimitriou, “Hierarchical Bayesian model updating for structural identification,” *Mechanical Systems and Signal Processing*, vol. 64-65, pp. 360–376, 2015. [Online]. Available: https://www.sciencedirect.com/science/article/pii/S0888327015001545

[84] I. Behmanesh and B. Moaveni, “Accounting for environmental variability, modeling

errors, and parameter estimation uncertainties in structural identification," *Journal of Sound and Vibration*, vol. 374, pp. 92–110, 2016. [Online]. Available: https://www.sciencedirect.com/science/article/pii/S0022460X16002698

[85] Y. Tamura and S.-y. Suganuma, "Evaluation of amplitude-dependent damping and natural frequency of buildings during strong winds," *Journal of Wind Engineering and Industrial Aerodynamics*, vol. 59, no. 2, pp. 115–130, 1996. [Online]. Available: https://www.sciencedirect.com/science/article/pii/0167610596000037

[86] Q. Li, K. Yang, N. Zhang, C. Wong, and A. Jeary, "Field measurements of amplitude-dependent damping in a 79-storey tall building and its efects on the structural dynamic responses," *The structural design of tall buildings*, vol. 11, no. 2, pp. 129–153, 2002.

[87] Q. Li, K. Yang, C. Wong, and A. Jeary, "The effect of amplitude-dependent damping on wind-induced vibrations of a super tall building," *Journal of Wind Engineering and Industrial Aerodynamics*, vol. 91, no. 9, pp. 1175–1198, 2003.

[88] Y. Hui, Z. Liu, K. Guo, and Q. Yang, "A mathematical model of nonlinear aerodynamic damping for high-rise buildings," *Journal of Engineering Mechanics*, vol. 150, no. 5, p. 04024021, 2024.